An Automated System for Measuring Power Devices in *Ka*-Band

Bertrand Bonte, Christophe Gaquière, *Member, IEEE*, Eric Bourcier, G. Lemeur, and Yves Crosnier

***Abstract*— An active load–pull system is presented for measuring devices from 50–μm to 3-mm gatewidth in *Ka*-band. It can automatically scan the interesting area of the Smith chart. The system protects the tested devices because the impedance is presented at the output of the device only if the gate current is lower than a fixed value. Results are presented at 30 and 38 GHz on a pseudomorphic high electron-mobility transistor (PM-HEMT).**

***Index Terms*— Load–pull, microwave measurements, network testing, transistor.**

I. Introduction

POWER monolithic microwave integrated circuit (MMIC) design requires information about large-signal behavior and nonlinear models used in computer-aided design (CAD) software. One of the most commonly used methods to verify the nonlinear models and get the power performance of a device consists of load–pull measurements. Passive load–pull measurements suffer from the inherent losses of passive tuners, so it is impossible to simulate highly reflective impedances. Active load–pull systems can overcome these limitations.

Two principles of active load–pull are well known. The first one is based on the active loop technique. A part of the signal delivered by the output of the device-under-test (DUT) is taken with a coupler, amplified and phase shifted, and reinjected at the output of the device to simulate the load. A system based on this principle has been published by Demmler [1] with a covered frequency range from 1 to 50 GHz.

The other technique has been proposed by Takayama [2]. A single source is used and a 3-dB splitter permits simultaneously injecting a part of the signal at the input of the device and another part (amplified and phase shifted) at the output of the device. A tuner can be inserted at the input of the DUT. If this tuner exists, optimum source and load impedances are directly available (assuming the Rollet factor k to be greater than one), otherwise it is necessary to calculate the corrected data from the raw data. Our approach is similar to that of Poulin [3]. This on-wafer pulsed active load–pull system can measure 4-W devices over C-band. Coupat's system [4] permits measurements of highly mismatched transistors with a mismatched source at the output of the device to decrease the power, but its frequency capability does not exceed 18 GHz. Teeter [5] proposed a system in Ka-band, but without any automation, and recently, Gao [6] has published an on-wafer load–pull system from 1 to 60 GHz. Finally, an active load–pull system based on the six-port technique has been published by Ghannouchi [7].

We have developed a new active load–pull bench based on the Takayama principle. It differs from the other systems in the following ways.

1) The WR28 waveguide structure allows high power density and limits the bandwidth to Ka-band, but benefits from the very high directivity of the reflectometer couplers.
2) The system can determine small- and large-signal scattering parameters or active load–pull measurements for devices having 50-μm to several-mm gatewidth without any modification.
3) All the measurements are fully automated and the area of interest of the Smith chart can be automatically scanned.
4) The impedance is presented at the output of the device only if the gate current is less than 1 mA/mm.

Indeed, it has been proven that gate current is the main limitation of the power capability, particularly for very small gate-length devices [8]. Thus, a limitation of the gate–current density is always fixed in order not to degrade the DUT. Due to the bandwidth of the system (from 26 to 40 GHz), no harmonic termination can be controlled. In fact, it is very difficult to set up a system which can operate both with fundamental frequency in *Ka*-band and harmonics. To our knowledge, any result has been published with harmonic control in this frequency range. Moreover, this point is less important than at lower frequency because the DUT may not be as efficient in generating harmonics.

Two other characteristics can be added. There is no tuner at the input of the DUT. Such a choice avoids oscillation of the device in *Ka*-band because the source impedance is then always 50 Ω. The measurement four-port system is a Wiltron 3630 down converter coupled with a Wiltron 360 vector network analyzer (VNA).

We will explain the structure of our system in Section II. Section III concerns calibration procedures which are fundamental in receiving accurate measurements. The automation of the system is explained in Section IV, and results are given in Section V.

II. Description of the System

The block diagram of the system is represented in Fig. 1. In network analyzer configuration, the RF signal is injected

Manuscript received January 6, 1997; revised October 9, 1997.

B. Bonte, C. Gaquière, E. Bourcier, and Y. Crosnier are with the Institut d'Électronique et de Microélectronique du Nord UMR-CNRS 9929, Département Hyperfréquences et Semiconducteurs, 59652 Villeneuve D'Ascq Cedex, France (e-mail: bonte@iemn.univ-lille1.fr).

G. Lemeur is with Thomson RCM, La clef Saint-Pierre, 78852 Elancourt, France.

Publisher Item Identifier S 0018-9480(98)00626-7.

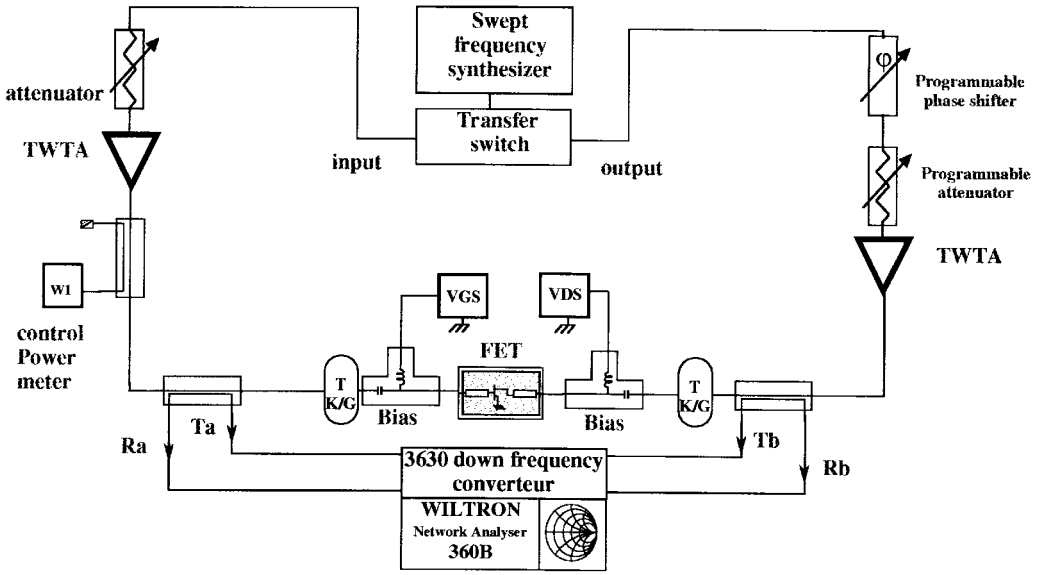

Fig. 1. Block diagram of the system.

alternately to the input and the output of the DUT with the other port loaded by 50 Ω. The DUT is placed in a test fixture with K-connectors. This one is based on the Dambrine principle [9]. It contains an insert between two half cells. In active load–pull configuration, the RF signal is simultaneously injected to the input and the output of the DUT. The transfer switch is the key component of our system; it allows use of this bench either as a VNA or as an active load–pull system. Usually, the transfer switch is included in a test set. It allows injecting the signal at one port of the DUT and terminating the other port with a 50-Ω impedance. The switching is controlled by the VNA. In our case, this transfer switch is outside the down converter and can be set in S-parameter configuration or in active load–pull configuration by replacing the two terminal 50-Ω load by an RF jumper (coaxial guide that links two terminations [10]).

A synthesizer has been chosen as the RF source due to its high-frequency stability and the wide frequency range of use. It allows very accurate calibration, and can be driven (in the case of low RF power) owing the external 10-MHz signal which phase locked the system (specific set on procedure of the VNA Wiltron 360). This system allows us to measure small gatewidth devices (50-μm) and highly mismatched large gatewidth devices ($>$ 1 mm) under linear and nonlinear operation without changing anything in the system. The system has been built in such a way as to obtain maximum RF power and a large dynamic range. Concerning the maximum RF power, our requirements lead to the choice of two 10-W tunneling wave tube amplifier (TWTA), so there is no problem for measuring unprematched devices. Moreover, there is no risk of oscillation of the device in the *Ka*-band because the source termination is 50 Ω. Each TWTA is connected to a *Ka*-band circulator so the input of the device is always closed to matched terminations avoiding oscillation.

The down converter is a Wiltron 3630 plug in, the linear operating range of the mixers is from -10 to -55 dBm. Consequently, the dynamic range is 45 dB.

The waveguide couplers allow a higher density power than coaxial couplers and present a better directivity. The phase shifter and attenuator can be manually or automatically driven (using an internal processor and a general-purpose interface board (GPIB) monitoring). The attenuator has 60-dB dynamic, with a step of 0.1 dB. The whole phase shifting is 720°, with a step of 0.2°. Both components have good reproducibility and speed (less than 1 s for all the dynamic). There is no problem of power level because the attenuator and phase shifter are both located at the input of the TWTA.

III. Calibration of the System

This point is crucial to be sure to get accurate results. Systematic errors are taken into account with calibration, but surrounding drifts are minimized by placing the system in a constant temperature room. Because of the two possibilities of the system (S-parameters and active load–pull measurements), two tiers are necessary in the calibration procedure. The first one concerns the impedance calibration, which is valid for the two functions of the system. In fact, if looking at the flow graphs of the S-parameters and load–pull configurations, the systematic error coefficients are identical. However, the equations needed to determine the corrected quantities are different. The second step is the power calibration for measuring the absolute power level at the input of the device.

A. The Impedance Calibration

Two methods were available to determine the error coefficients. The first one uses a cascade of two tiers and consists of doing a short open load thru (SOLT) calibration to calibrate the VNA, and then cascading the test fixture. In the second method, a thru reflect line (TRL) calibration is performed. With the second method, only one step is necessary because the entire system (VNA + fixture) is calibrated.

A comparison of the two methods indicates that the second method is better. However, an advantage of the first method

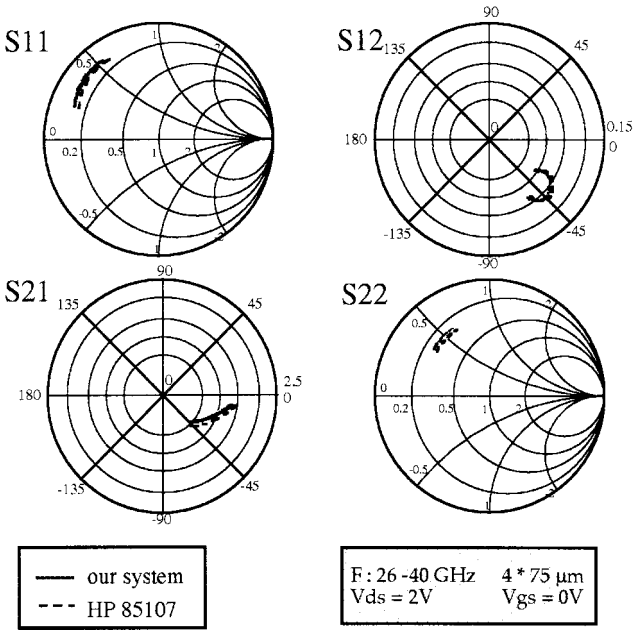

Fig. 2. Comparison of the measured scattering parameters with our system and a classical network analyzer (HP 85 107).

is to allow separate measurements of the half fixture, which is necessary for the power calibration.

Concerning the S-parameter measurements, typical flow graphs can be drawn in forward and reverse configurations. S-parameters are deduced from raw S-parameters using a set of equations that can be found in [11].

Another set of equations has been written for the load–pull configuration to complete the impedance calibration procedure.

In order to validate this calibration, the same device FET was measured in the whole band with our system and using a standard VNA (HP85107). A very good agreement between the two measurements was obtained for each scattering parameter (Fig. 2), leading to the conclusion that calibration and measurements exhibit good accuracy.

B. The Power Calibration

To reach a very good accuracy in the measurements, the power correction method is not scalar corrected, but vector corrected. The first step consists of the measurement of the injected power to the K cell input plane with a power meter (to obtain an absolute power level), under the $a_{1m}/1$ procedure. A one-port calibration is also done with the Wiltron 360B in this plane to determine the error terms e'_{00}, e'_{11}, and $e'_{10}e'_{01}$, as shown in Fig. 3. The reflected coefficient Γ_ε of the power probe is also measured. According to the flow graph of this configuration, it is possible to extract the magnitude of e'_{10} term using the following equations:

$$a'_1 = \frac{e'_{10}a_{1\mathrm{m}}}{1 - e'_{11}\Gamma_\varepsilon}$$
$$P_\varepsilon = |a'_1|^2(1 - |\Gamma_\varepsilon|^2)$$

which lead to

$$|e'_{10}|^2 = \frac{P_\varepsilon |1 - e'_{11}\Gamma_\varepsilon|^2}{|a_{1\mathrm{m}}|^2(1 - |\Gamma_\varepsilon|^2)}$$

where P_ε is the probe absorbed power.

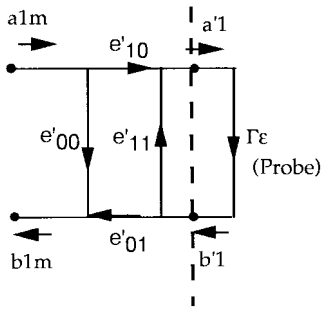

Fig. 3. Flow graph used for the first part of the power calibration in load–pull configuration.

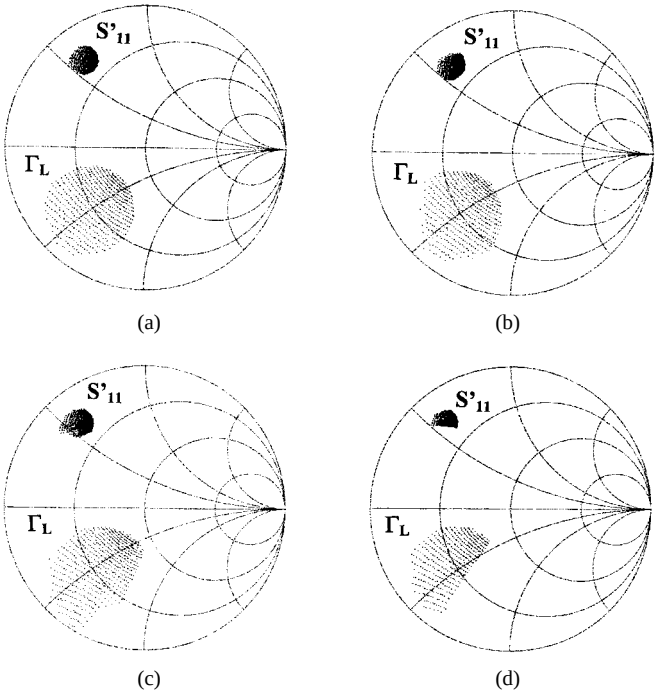

Fig. 4. Evolution of the scanned area in the Smith chart for four injected input power levels. (a) 5.5 dBm. (b) 7.5 dBm. (c) 11 dBm. (d) 11.6 dBm. S'_{11} and Γ_L are represented.

The second step concerns the true measurement configuration of the DUT, which implies the insertion of the input half K cell. A correction is necessary to obtain the true injected power P_1 to the DUT input plane. This correction is realized using the error terms of the input half K cell determined previously and the source mismatch. Finally, the incident wave a_1 and the corresponding incident power P_1 can be obtained using the following:

$$a_1 = \frac{e'_{10}e_{01}a_{1m}}{1 - e'_{11}e_{00} - e_{11}s'_{11} + e_{11}e'_{11}e_{00}s'_{11} - e_{10}e_{01}e'_{11}s'_{11}}$$
$$P_1 = \frac{|e'_{10}|^2\,|e_{01}|^2\,P_{1mes}}{|1 - e'_{11}e_{00} - e_{11}s'_{11} + e_{11}e'_{11}e_{00}s'_{11} - e_{10}e_{01}e'_{11}s'_{11}|^2}$$

where S'_{11} is the reflection coefficient in the DUT input plane. In the P_1 expression the quantity $|e_{01}|^2$ is basically unknown. Nevertheless, assuming that the half K cell (because of its simplicity) behaves approximately like a reciprocal network, the $|e_{01}|^2$ quantity may be replaced by the product $|e_{01}e_{10}|$.

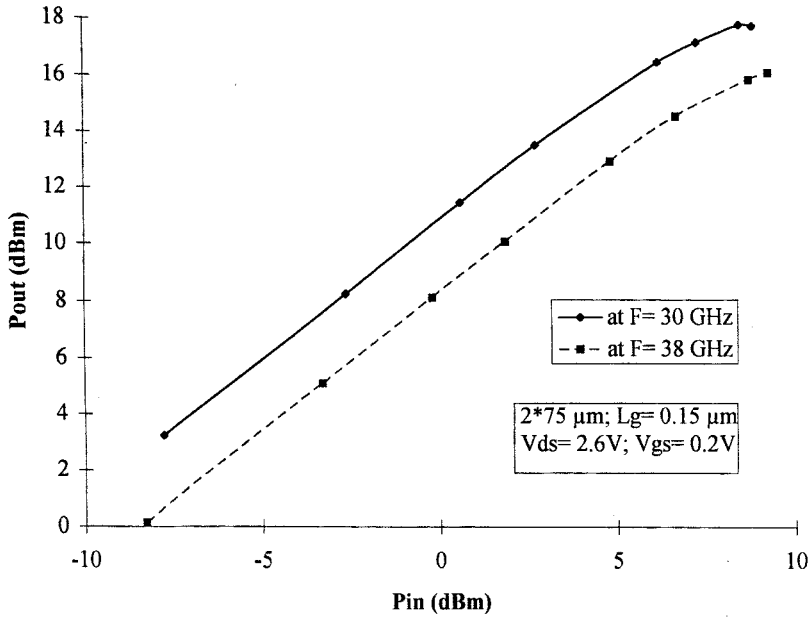

Fig. 5. Power response of the device at 30 and 38 GHz.

At this stage of the procedure, it is then possible to determine all the injected and absorbed power level at the input and output of the DUT.

IV. Automation of the System

To our knowledge, the procedure that has been established to fully characterize a device is the first one to provide so much convenience and safety. The requirement of a full automation of the system is made necessary for two main reasons. The first concerns time saving and the second concerns the device failure (i.e., avoiding oscillations and high gate–current areas). The Labwindow CVI software (National Instrument trademark) has been chosen for driving the elements of the system (ammeter, dc power supply, attenuator, power meter, phase shifter, and the VNA).

The "standard" procedure for a full characterization of a device consists of initially measuring its scattering parameters. After this first step, the operator can choose between continuing large-signal scattering-parameter measurements only by increasing the RF signal level or placing the system in the active load–pull configuration by changing the 50-Ω load of the transfer switch by an RF jumper. Using a computation of the data recorded before (small-signal S-parameters), it is possible to determine the interesting area in the Smith chart in order to avoid the zones where the device is passive or unstable. For example, the tested area could correspond to a given power gain chosen by the operator. Moreover, this procedure greatly reduces the number of recorded data.

When the studied area has been fixed, the phase shifter and attenuator are programmed using the front-end panel of the CVI software. The interesting area is scanned for each input power level, with a variation of the attenuator at each point of measurement. The phase shifter only changes when the impedance is at the edge of the interesting area.

If the gate current is very low (at low-input power level), the only limitation of the described area will be the equation of the minimum gain circle chosen by the operator. However, if the gate current is high (commonly 1 mA/mm), it is necessary to know before a new impedance is settled whether or not the gate current at this new impedance will be greater than the damage limit of the DUT. The procedure that has been established consists of a test on the gate current at the previous impedance or at the previous power level. If the gate current at impedance i is less than 90% of the limit, the impedance $i+1$ can be presented at the output of the device without any problem. In the other case, a test will be done in the previous file (corresponding to the previous input power level) to check the value of the gate current and its variation rate. Depending on the result of this test, the impedance $i+1$ is or is not electrically simulated.

The safety of the above procedure has been checked using several kind of devices. No degradation or failure was noted. Typical examples of results are presented in the next section.

V. Results

When the transistor is mounted in its test fixture, 8 h are necessary to automatically and fully characterize the device under power conditions. The number of simulated impedances is around 1000 for each power level with approximately 10 injected power levels at the input of the device.

The device presented in this paper is a pseudomorphic high electron-mobility transistor (PM-HEMT) with 0.15-μm gate length and a single δ-doped plane of 5.10^{12} at/cm^2 density. The total gatewidth is 2*75-μm. Measurements have been performed at 30 and 38 GHz, the biasing point is $V_{\rm ds} = 2.6$ V and $V_{\rm gs} = 0.2$ V (i.e., in class A).

Fig. 4 shows the studied area on the Smith chart for four injected power levels. Following S-parameter measurements, the interesting area has been determined, as shown in Fig. 4(a)

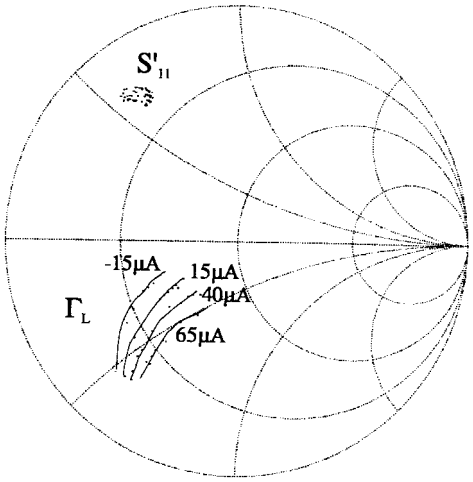

Fig. 6. Representation of the iso-gate–current curves in the Smith chart.

(the criterion in this example is a power gain higher than 9 dB in the entire area). When the injected power level increases, this area is automatically reduced to avoid the high gate–current region [Fig. 4(a)–(d)]. From a given injected power level to the next, the shape of the area of interest can be modified in various manners depending on the value taken by the average gate current. Compression level is 1.5 dB in case c, and 2 dB in case d. Beyond this level, the scanned area is too small due to the high gate current, and results are not significant.

The power response has been performed at 30 and 38 GHz, without changing anything in the system. The results are drawn in Fig. 5. Maximum power densities are 380 and 265 mW/mm at 30 and 38 GHz, respectively, with corresponding power-added efficiency of 40% and 26%.

During measurements, the gate current is recorded and curves corresponding to "equi-gate current" can be drawn in the Smith chart (Fig. 6). These curves concern either forward or reverse gate–current cases, but the optimum load corresponds roughly to the lower level gate–current area. This property is typical of optimum power behavior and has been checked on many PM-HEMT's [12].

Finally, Fig. 7(a) indicates the power-gain circles under linear conditions and shows those (b) under high-level conditions. The optimized impedance changes and the maximum gain is only 9.5 dB at 2.5-dB compression. It is important to note that curves do not describe whole circles in the second case because of the gate–current limitation that was imposed during measurements. Thus, it is possible to increase the acceptable gate–current value and to depict all the noncircular contour.

VI. Conclusion

A 26–40 GHz automated active load–pull system has been presented. In a first configuration, it permits measuring scattering parameters in small- and large-signal conditions. In the other configuration, it permits extracting all gains, power levels, impedances of interest, average currents, and efficiencies for a given device, even for very large gatewidth. The new automated procedure avoids impedances that could result in device degradation.

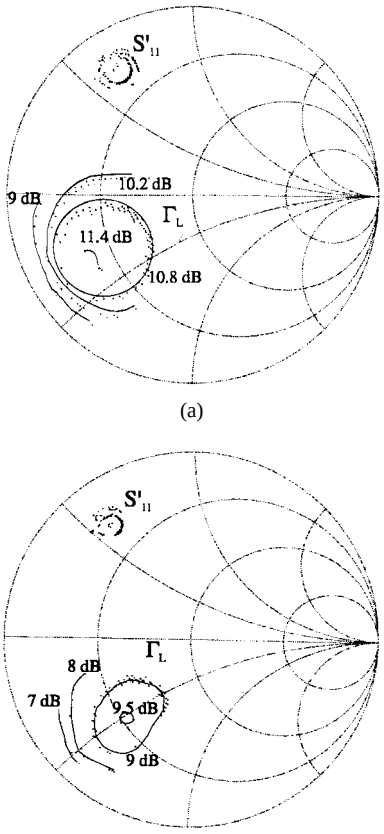

Fig. 7. Representation of the constant power-gain circles in the Smith chart for two injected input power levels corresponding to (a) the linear condition and (b) the large signal condition.

Acknowledgment

The authors would like to thank Y. Mancuso from Thomson RCM, Elancourt, France, and F. Grossier from Wiltron, Courtaboeuf, France, for helpful discussions.

References

[1] M. Demmler, B. Hughes, and A. Cognata, "A 0.5–50 GHz on wafer, intermodulation, load–pull and power measurement system," in *IEEE-MTT-S Int. Microwave Symp. Dig.*, Orlando, FL, May 1995, pp. 1041–1044.

[2] Y. Takayama, "A new load pull characterization method for microwave power transistors," in *IEEE-MTT-S Int. Microwave Symp. Dig.*, 1976, pp. 218–220.

[3] D. Poulin, J. Mahon, and J. P. Lanteri, "A high power on-wafer pulsed active load pull system," *IEEE Trans. Microwave Theory Tech.*, vol. 40, pp. 2412–2417, Dec. 1992.

[4] P. Bouysse, J. M. Nebus, J. M. Coupat, and J. P. Villotte, "A novel, accurate load pull setup allowing the characterization of highly mismatched power transistors," *IEEE Trans. Microwave Theory Tech.*, vol. 42, pp. 327–332, Feb. 1994.

[5] D. Teeter, J. East, R. Mains, and G. Haddad, "Large signal characterization and numerical modeling of the GaAs/GaAlAs HBT," in *IEEE-MTT-S Int. Microwave Symp. Dig.*, Boston, MA, June 1991, pp. 651–654.

[6] Y. Gao, D. Kother, B. Roth, T. Sporkmann, and I. Wolff, "Improvements in on wafer load pull measurements," in *25th European Microwave Conf.*, Bologna, Italy, Sept. 1995, pp. 334–338.

[7] F. Ghannouchi and R. Bosisio, "An automated millimeter-wave active load-pull measurement system based on six-ports techniques," *IEEE Trans. Instrum. Meas.*, vol. 41, pp. 957–962, June 1992.
[8] C. Gaquière, D. Théron, B. Bonte, and Y. Crosnier, "1 W/mm power pseudomorphic HFET with optimized recess technology," *Inst. Elect. Eng. Electron. Lett.*, vol. 30, no. 11, pp. 904–906, May 1994.
[9] G. Dambrine, A. Cappy, F. Héliodore, and E. Playez, "A new method for determining the FET small signal equivalent circuits," *IEEE Trans. Microwave Theory Tech.*, vol. 36, pp. 1151–1159, July 1988.
[10] C. Gaquière, E. Bourcier, B. Bonte, and Y. Crosnier, "A novel 26–40 GHz active load pull system," in *25th European Microwave Conf.*, Bologna, Italy, Sept. 1995, pp. 339–342.
[11] J. Williams, "Accuracy enhancement fundamentals for vector network analyzers," *Microwave J.*, pp. 99–114, Mar. 1989.
[12] C. Gaquière, B. Bonte, E. Bourcier, and Y. Crosnier, "Correlation between gate current and RF power performances of millimeter HEMT's," in *26th European Microwave Conf.*, Prague, Czech Republic, Sept. 1996, pp. 33–36.

Bertrand Bonte was born in Roubaix, France, in 1963. He received the Dipl.Eng. degree from the Institut Supérieur d'Electronique du Nord, Lille, France, in 1986, and the Ph.D. degree in electrical engineering from the University of Lille, Lille, France, in 1990.

He is currently Maître de Conférences at the University of Lille. His research concerns the small-signal characterizations, breakdown behavior, and the power measurements of heterostructure FET's at millimeter-wave frequency. He is also involved in the MMIC design activities of the Institut d'Électronique et de Microélectronique du Nord (IEMN), Cedex, France.

Christophe Gaquière (S'94–A'95–M'96) was born in Bailleul, France, in 1966. He received the Dipl. d'Etudes Supérieures Spécialisées en Microélectronique and the Ph.D. degrees in electronics from the University of Lille, Lille, France, in 1990 and 1995, respectively.

He is currently Maître de Conférences at l'Ecole Universitaire d'Ingénieur de Lille (EUDIL), Lille, France, and carries out his research activity at the Institut d'Électronique et de Microélectronique du Nord (IEMN).

His areas of interest are GaAs and InP-based HEMT's, and circuits (hybrid or MMIC) for millimeter-wave applications. He is involved in the characterization of these devices under small- or large-signal conditions. He studies the breakdown behavior in correlation with the epilayers and recess topologies, and has developed instrumentation system in the Ka-band.

Eric Bourcier was born in Saint-Quentin, France, on February 16, 1970. He received the Diplome d'Etudes Approfondies en Electronique from the University of Lille, Lille, France, in 1993, and is currently working toward the Ph.D. degree. His subject of interest is the investigation of measurements of HEMT's and PHEMT's on InP and GaAs for power application with an active load–pull system in Ka-band.

G. Lemeur, photograph and biography not available at time of publication.

Yves Crosnier was born in Roubaix, France, in 1937. He received the doctorate degree in electronics and the state doctorate degree from the University of Lille, Lille, France, in 1963 and 1973, respectively.

In 1975, he joined the Microwave and Semiconductors Laboratory, University of Lille, Département Hyperfréquences et Semiconducteurs (DHS), Institut d'Électronique et de Microélectronique du Nord (IEMN), where he is currently Professor and Head of a research team working on modeling, analysis, and applications of microwave field-effect transistors, especially in the field of power amplification and nonlinear devices.